Braz J Phys (2013) 43:152–161
DOI 10.1007/s13538-013-0127-0

SOCIEDADE BRASILEIRA DE FÍSICA

NUCLEAR PHYSICS

# Study of Alpha Decay Chains of Superheavy Nuclei and Magic Number Beyond $Z = 82$ and $N = 126$

**Shagun Thakur · Sushil Kumar · Rajesh Kumar**

Received: 12 September 2012 / Published online: 11 April 2013


**Abstract** We study various $\alpha$-decay chains on the basis of the preformed cluster decay model. Our work targets the superheavy elements, which are expected to show extra stability at shell closure. Our computations identify the following combinations of proton and neutron numbers as the most stable nuclei: $Z = 112$, $N = 161, 163$; $Z = 114$, $N = 171, 178, 179$; and $Z = 124$, $N = 194$. We also investigate the alternative of heavy cluster emissions in the decay chain of $^{301}120$, instead of $\alpha$ decay. Our study of cluster radioactivity shows that the half-life for $^{10}$Be decay in $^{289}114$ is larger, indicating enhanced stability at $Z = 114$, $N = 175$. Similar calculations concerning the emission of $^{14}$C and $^{34}$Si from $^{301}120$ find the more stable combinations $Z = 114$, $N = 173$, and $Z = 106$, $N = 161$, respectively. From the same parent, $^{301}120$, the emission of a $^{49-51}$Ca cluster yielding a $Z = 100$, $N = 152$ daughter is the most probable.

**Keywords** Half-life · Cluster decay · SHE

## 1 Introduction

The quest for the next magic numbers, beyond the doubly magic nucleus $^{208}$Pb, has long been with us. A number of theoretical efforts [1–9] were made in the late 1960s in search of long-lived superheavy nuclei. The proton numbers $Z = 114$, 124, and 164 were predicted, along with the neutron numbers $N = 184$, 196, 236, and 318. On the basis of Strutinsky's approach, certain models have found $Z = 114$ to be the most stable [10–12], whereas models based on Hartree–Fock calculations associate $Z = 120$, 124, and 126 with the highest stability [13, 14]. The combination $Z = 120$ and $N = 172$ was predicted to be doubly magic [15, 16].

Recent calculations based on the newly proposed isospin cluster model have also identified $N = 172$ as a magic number [17]. Adamian et al. [18] studied evaporation-residue cross sections to conclude that the next magic nucleus beyond $^{208}$Pb would have $Z \geq 120$. Very recently, however, Zhang et al. have argued that $^{270}$Hs, with $Z = 108$ and $N = 162$, is the next sub-magic nucleus and that $^{298}114$, with $Z = 114$ and $N = 184$ is a spherical doubly magic nucleus [19]. Our earlier research [20] also indicated higher stability for $Z = 108$ with $N = 162$. In addition, we have found that the pairs $Z = 115$, $N = 172$; $Z = 113$, $N = 170$; and $Z = 107$, $N = 165$ are also more stable, due to the magicity of $Z = 114$, $N = 172$. Here, we extend our work to study the stability of superheavy elements in different nuclear zones.

The synthesis of the superheavy elements has received a fillip from advances in accelerator technology. During the last two decades, a great deal of experimental data concerning superheavy elements have been gathered. Superheavy elements have been synthesized in cold and hot fusion reactions. The superheavy elements with $Z = 107 - 112$ have been synthesized with lead and bismuth targets in cold fusion reactions [21], whereas the elements with $Z = 114$ [22, 23], 116 [24], and 117 [25] have been identified in hot fusion reactions. The latter use heavy actinide targets, from Th to Cf, and very light projectiles, from C to S. A neutron-rich beam of $^{50}$Ca projectiles has proved more

S. Thakur (✉) · R. Kumar
Department of Physics,
National Institute of Technology-Hamirpur, 177005 Hamirpur, India
e-mail: shagunnitham@gmail.com

S. Kumar
Chitkara University-Solan, 174103 Solan, India

appropriate in cold fusion-based syntheses of superheavy elements [26, 27]. Recently, Zagrebaev et al. have discussed transfer reactions [28] and neutron capture reactions [29] for the production of superheavy nuclei. The decay of such nuclei starts with a sequence of $\alpha$ particles [30, 31] and ends with spontaneous fission. Each isotope has its own characteristic chain of sequential $\alpha$ emission, which identifies the synthesized superheavy elements. Alternative, exotic decay modes of these superheavy nuclei, such as cluster (heavy-ion) radioactivity [32, 33] and ternary fission [34] have also been investigated recently.

Since superheavy nuclei would not exist without shell stabilization, shell effects have been intensively studied in such nuclei. So far, only neutron-deficient superheavy isotopes have been prepared. The experimental information concerning neutron-rich isotopes is therefore scarce, a circumstance that highlights the importance of understanding the available data, studying different synthesis reactions, and analyzing the stability of different $Z$, $N$ combinations in the superheavy mass region. With this in mind, we have investigated the experimentally observed decay chains of $^{288,287}115$ nuclei [20] on the basis of the preformed cluster model (PCM), due to Gupta and collaborators [35–39]. Given the current debate on whether $Z = 120$ is a magic number and the attempts to synthesize it, we here extend of our work. To probe the stability of nuclei beyond $Z = 115$, we analyze $\alpha$ decay chains of various $Z = 120$ isotopes. In addition, we consider two long chains of $^{326,320}128$ nuclei. For $^{301}120$, besides $\alpha$ decay, we examine the emission of heavy clusters.

A brief description of the PCM is presented in Section 2. Our results are presented in Section 3 and compared with recent model calculations. A summary of our results is presented in Section 4

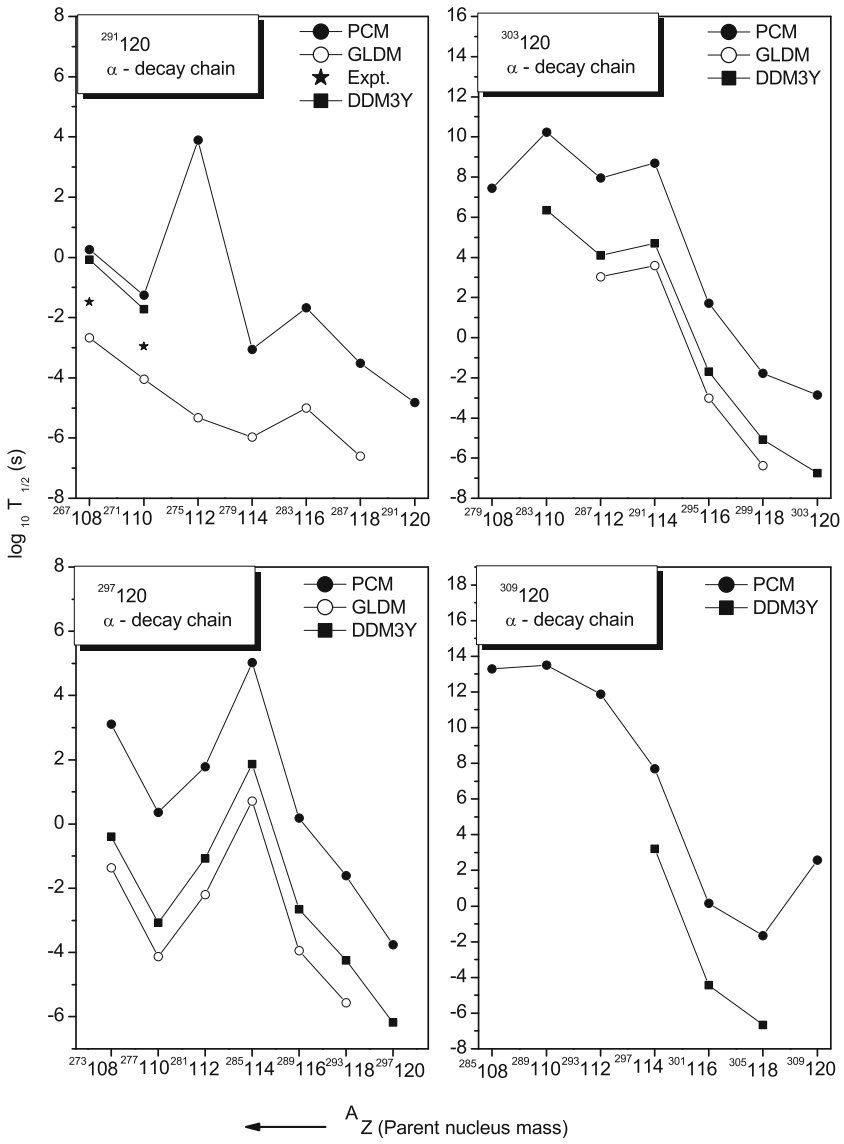


**Fig. 1** Alpha decay half-lives for the PCM as a function of the parent nucleus' mass for the alpha decay chains of $^{291,297,303,309}120$, compared with the available experimental data [22–25, 54]. Also shown are the half-lives calculated on the basis of the GLDM and DDM3Y models [53]

## 2 Preformed Cluster Model

Details of the PCM, upon which our calculation are based, can be found in [20] and references therein. In the PCM, the dynamical collective coordinates

$$\eta = (A_1 - A_2)/(A_1 + A_2) \tag{1}$$

and

$$\eta_Z = (Z_1 - Z_2)/(Z_1 + Z_2) \tag{2}$$

represent the mass and charge asymmetries, respectively, where the subindices 1 and 2 denote the heavier and lighter fragments, respectively.

The collective coordinates, first introduced in quantum mechanical fragmentation theory [40–45], are additional to the usual coordinates, namely, the relative separation $R$ of the fragments and deformations $\beta$ of the involved nuclei. With the standard approximation, which decouples the motion associated with $R$ from that associated with $\eta$ [35, 36, 47, 48], the decay constant $\lambda$ and the half-life $T_{1/2}$ in the PCM are given by the relation

$$\lambda = \frac{ln2}{T_{1/2}} = P_0 \nu_0 P, \tag{3}$$

where $P_0$ is the cluster preformation probability, $P$ is the barrier penetrability, and $\nu_0$ represents the barrier assault frequency.

To calculate the probability $P_0$, one solves the stationary Schrödinger equation in the $\eta$ coordinate at fixed $R = R_a = C_t(= C_1 + C_2)$, where the $C_i$ are the Süssmann central radii $C_i = R_i - (1/R_i)$, with $R_i =$

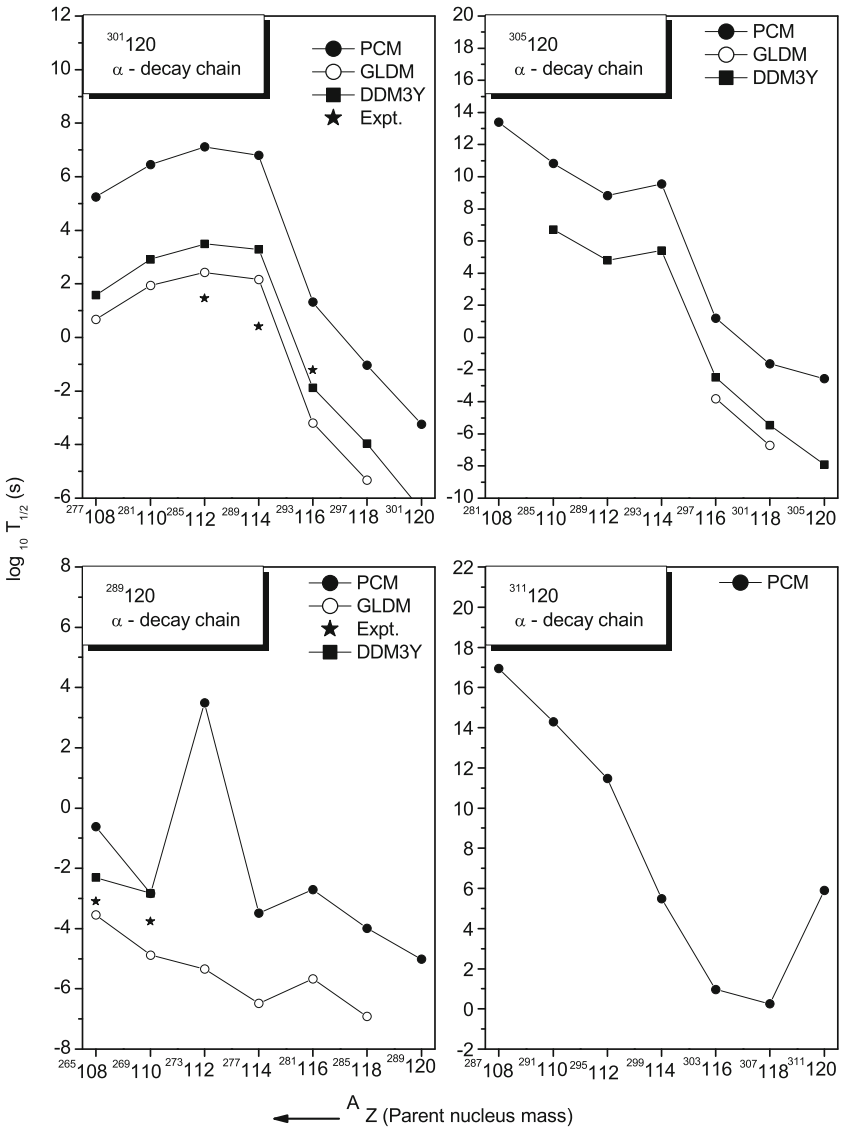


**Fig. 2** Alpha decay half-lives for the PCM plotted as a function of the parent nucleus' mass for the alpha decay chains of $^{301,305,289,311}$120, compared with the available experimental data [22–25, 54]. Also shown are the half-lives computed for the GLDM and DDM3Y [53]

$1.28A_i^{1/3} - 0.76 + 0.8A_i^{-1/3}$fm. Upon normalizing the solutions, one finds that

$$P_0 = \sqrt{B_{\eta\eta}} \mid \psi^{(0)}(\eta(A_i)) \mid^2 (2/A)\,, \tag{4}$$

with $i = 1, 2$ and $\nu = 0, 1, 2, 3, \ldots$.

The fragmentation potential in the Schrödinger equation is the sum of the Coulomb interaction, the nuclear proximity potential [49], and the ground-state binding energies of two nuclei:

$$V(R_a, \eta) = -\sum_{i=1}^{2} B(A_i, Z_i) + \frac{Z_1 Z_2 e^2}{R_a} + V_P, \tag{5}$$

with the $B$'s taken from the 2003 experimental compilation by Audi and Wapstra [50] and, for those not available in [50], from the 1995 calculations by Möller et al. [51]. Shell effects directly obtained from measured or calculated binding energies are therefore fully included in the calculations.

Minimization of the potential with respect to the $\eta_Z$ coordinate fixes the effective charges $Z_1$ and $Z_2$ on the right-hand side of Eq. (5). The Coulomb and proximity potentials are obtained from spherical nuclei. The mass parameters $B_{\eta\eta}$ in Eq. (4) are the classical hydrodynamical masses [52]. The shell effects in the masses have been shown [48] not to affect the calculated yields within the accuracy of the approximation.

To calculate the penetration probability $P$, one relies on the Wentzel-Kramers-Brillouin (WKB) approximation for the barrier tunnelling probability. More specifically, the probability is $P = P_i P_b$, where $P_i$ and $P_b$ are calculated analytically from standard WKB integrals [35]. The second turning point $R_b$ is chosen so that $V(R_b)$ be equal to the $Q$ value for ground-state decay.

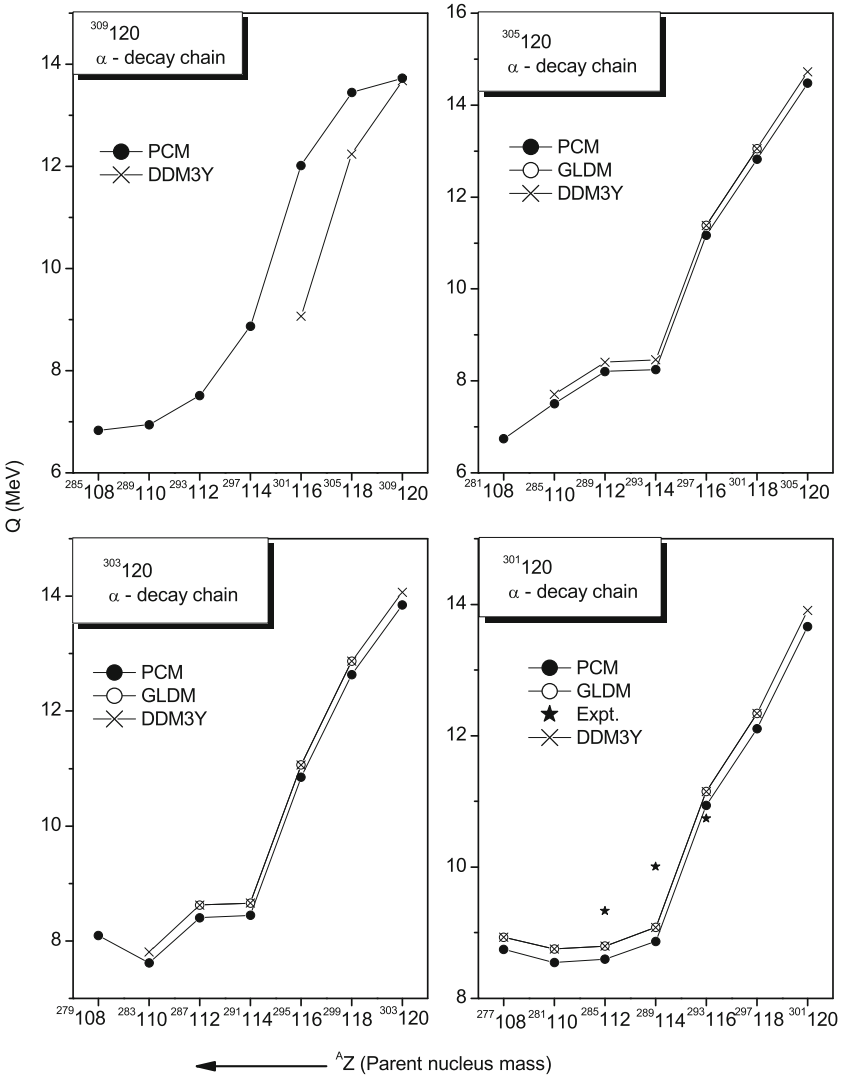


**Fig. 3** Alpha decay energies $Q_\alpha$ for the PCM, as a function of the parent nucleus' mass for the alpha decay chains of $^{309,305,303,301}120$, compared with the available experimental data [22–25, 54]. Also shown are the energies for the GLDM and DDM3Y [53]

The assault frequency $\nu_0$ in Eq. (3) is simply given by the equality

$$\nu_0 = (2E_2/\mu)^{1/2}/R_0, \tag{6}$$

where $E_2 = (A_1/A)Q$, the kinetic energy of the lighter fragment, for the $Q$ value shared between the two products, in inverse proportion to their masses.

## 3 Calculations

### 3.1 The $\alpha$ Decay Chain in Superheavy Nuclei

Proton and neutron shell effects make nuclei more stable. The stronger the shell effects, the longer the half-life of the nucleus. In our calculations, we have investigated the stability of superheavy nuclei by focusing on the shell effects. We have studied ten chains of $\alpha$ decay of $^{289,291,297}120$, $^{301,303,305,309,311}120$, and $^{320,326}128$ nuclei. We compare the results with Royer and Gherghesu's [53] computation for the generalized liquid-drop model (GLDM) and the DDM3Y model [53], and with experimental data [22–25, 54].

The trends of our results match those of the two previous model calculations. The computed half-lives are shown in Figs. 1 and 2. The maximum half-lives of the $\alpha$ decay chains $^{289,291,297}120$ correspond to the ground-state configurations of nuclei with $Z = 112$, $N = 161$; $Z = 112$, $N = 163$; and $Z = 114$, $N = 171$.The enhanced stability at neutron numbers 161 and 163 can be identified with $N = 162$, a deformed magic number [55]. Similarly, the element $Z = 114$, $N = 171$ is more stable against $\alpha$ decay. This seems to be associated with the proton number $Z = 114$, predicted to be a magic number along with $N = 184$. The neutron number 171 is close to $N = 172$, predicted to be magic number with $Z = 120$ by Rut et al., who scanned a wide

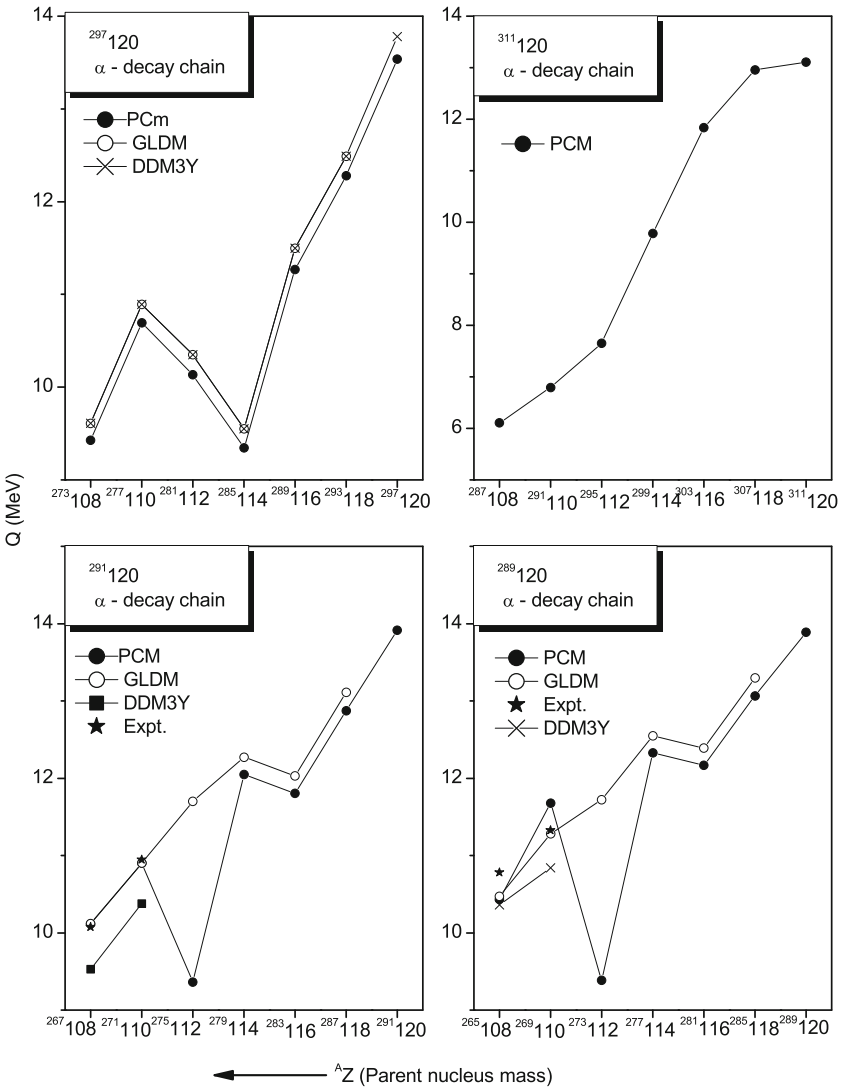


**Fig. 4** Alpha decay energies $Q_\alpha$ for the PCM as a function of parent nucleus' mass for the alpha decay chains of $^{297,311,291,289}120$, compared with the available experimental data [22–25, 54]. Also shown are the energies for the GLDM and DDM3Y [53]

**Table 1** $\alpha$ decay half-lives ($log_{10}T^{\alpha}_{\frac{1}{2}}(s)$) and other characteristic quantities for ground-state decays of superheavy nuclei with $Z = 108 - 118$ calculated for the PCM, compared with Dubna data for the $\alpha$-particle energies $E_\alpha$ and decay times $\tau$, which are interpreted as $Q_\alpha^{\text{expt}}$ and $T^{\alpha}_{\frac{1}{2}}$, respectively, and with GLDM calculations. For the PCM, the calculations are carried out at $R_a = C_1 + C_2 = C_t$, with binding energies from Audi-Wapstra and Wapstra [50] and Möller et al. [51]. Increasing or decreasing $R_a$ leads to no improvement in the PCM results

| Parent | PCM | | | | GLDM | | DDM3Y | | Experiments | |
|---|---|---|---|---|---|---|---|---|---|---|
| | $Q_\alpha$ (MeV) | $-Log\,P_0$ | -LogP | $log_{10}T^{\alpha}_{\frac{1}{2}}$ (s) | $Q_\alpha$ (MeV) | $log_{10}T^{\alpha}_{\frac{1}{2}}$ (s) | $Q^{MS}_{th}$ (MeV) | $log_{10}T^{\alpha}_{\frac{1}{2}}(Q^{MS}_{th})$ (s) | $E_\alpha$ (MeV) | $log_{10}\tau$ (s) |
| $^{294}118$ | 8.561 | 7.392 | 20.626 | 6.446 | 12.51 | −5.60 | 12.51 | −4.66 | 11.81 | −2.745 |
| $^{293}118$ | 12.301 | 11.012 | 12.629 | 1.991 | 12.49 | −5.56 | 12.49 | −4.24 | | |
| $^{294}117$ | 8.964 | 10.224 | 19.105 | 7.7484 | 11.90 | −4.62 | 11.90 | −2.88941 | 10.81 | 0.077616 |
| $^{293}117$ | 8.373 | 6.7055 | 20.914 | 6.0526 | 11.91 | −4.63 | 11.91 | −3.456 | 11.03 | 0.014553 |
| $^{293}116$ | 8.887 | 8.176 | 19.033 | 5.63 | 11.15 | −3.19 | 11.15 | −1.883 | 10.67 | −2.276 |
| $^{292}116$ | 10.708 | 6.688 | 14.808 | −0.124 | 11.03 | −2.85 | 11.03 | −1.97 | 10.80 | −1.744 |
| $^{291}116$ | 11.001 | 7.888 | 14.290 | 0.551 | 11.33 | −3.57 | 11.33 | −2.28 | 10.89 | −2.201 |
| $^{290}116$ | 11.211 | 6.380 | 13.944 | −1.308 | 11.34 | −3.58 | 11.34 | −2.69 | 11.00 | −1.823 |
| $^{289}116$ | 11.701 | 11.156 | 13.182 | 2.696 | 11.50 | −3.94 | 11.50 | −2.65 | | |
| $^{290}115$ | 10.301 | 8.4584 | 15.398 | 2.2428 | 10.15 | −0.80 | 10.15 | 0.864 | 9.95 | 0.015939 |
| $^{289}115$ | 10.601 | 7.2007 | 14.827 | 0.40713 | 10.24 | −1.05 | 10.24 | 0.017 | 10.31 | 0.22176 |
| $^{288}115$ | 10.999 | 7.775 | 14.124 | 0.271 | 10.34 | −1.32 | 10.34 | 0.35 | 10.61 | −1.06 |
| $^{287}115$ | 11.301 | 10.352 | 13.636 | 2.353 | 10.48 | −1.68 | 10.48 | −0.598 | 10.74 | −1.495 |
| $^{289}114$ | 9.908 | 8.488 | 15.989 | 2.871 | 9.08 | 2.16 | 9.08 | 3.292 | 9.96 | 0.414 |
| $^{288}114$ | 9.97 | 7.211 | 15.87 | 1.473 | 9.39 | 1.16 | 9.39 | 1.90 | 10.08 | −0.097 |
| $^{287}114$ | 10.437 | 8.175 | 14.938 | 1.496 | 9.53 | 0.74 | 9.53 | 1.905 | 10.16 | −0.318 |
| $^{286}114$ | 10.701 | 6.656 | 14.462 | −0.506 | 9.61 | 0.51 | 9.61 | 1.262 | 10.33 | −0.886 |
| $^{285}114$ | 11.001 | 11.09 | 13.956 | 3.415 | 9.55 | 0.71 | 9.55 | 1.87 | 0.00 | 0.00 |
| $^{286}113$ | 9.681 | 8.8386 | 16.277 | 3.514 | 9.10 | 1.78 | 9.10 | 3.332 | 9.63 | 19.6119 |
| $^{285}113$ | 10.021 | 7.4389 | 15.56 | 1.3893 | 9.18 | 1.53 | 9.18 | 2.471 | 9.74 | 5.4747 |
| $^{284}113$ | 10.251 | 8.062 | 15.112 | 1.558 | 9.36 | 0.96 | 9.36 | 2.532 | 10.15 | −0.318 |
| $^{283}113$ | 10.601 | 9.767 | 14.469 | 2.613 | 9.56 | 0.35 | 9.56 | 1.312 | 10.26 | −1.000 |
| $^{282}113$ | 7.563 | 4.714 | 22.516 | 5.679 | 10.00 | −0.93 | 10.00 | 0.654 | | |
| $^{278}113$ | 9.65 | 8.869 | 16.468 | 3.731 | 12.77 | −7.15 | 11.625 | −3.378 | | |
| $^{285}112$ | 8.734 | 9.153 | 18.37 | 5.942 | 8.80 | 2.43 | 8.80 | 3.499 | 9.28 | 1.462 |
| $^{284}112$ | 9.302 | 7.799 | 16.922 | 3.127 | 8.89 | 2.13 | 8.89 | 2.79 | | |
| $^{283}112$ | 9.621 | 8.712 | 16.199 | 3.309 | 9.22 | 1.06 | 9.22 | 2.16 | 9.67 | 0.579 |
| $^{282}112$ | 9.961 | 4.627 | 15.387 | −1.596 | 9.62 | −0.16 | 9.62 | 0.539 | | |
| $^{281}112$ | 10.281 | 8.342 | 14.869 | 1.592 | 10.35 | −2.20 | 10.35 | −1.074 | | |
| $^{277}112$ | 11.623 | 9.429 | 12.76 | 0.542 | 12.30 | −6.551 | 12.30 | −5.496 | 11.59 | −1.16 |
| $^{282}111$ | 9.381 | 8.7825 | 16.497 | 3.682 | 9.00 | 1.42 | 9.00 | 2.935 | 9.00 | 0.51282 |
| $^{280}111$ | 9.981 | 8.197 | 15.236 | 1.821 | 10.34 | −2.48 | 10.34 | −0.966 | 9.87 | 0.556 |
| $^{279}111$ | 10.451 | 6.845 | 14.366 | −0.412 | 11.12 | −4.41 | 11.12 | −3.456 | 10.52 | −0.769 |
| $^{278}111$ | 10.721 | 4.583 | 13.768 | −3.278 | 11.59 | −5.42 | 11.59 | −3.95 | | |
| $^{274}111$ | 11.601 | 6.876 | 12.671 | −2.102 | 11.07 | −4.21 | 11.07 | −2.71 | 11.32 | −2.194 |
| $^{272}111$ | 11.443 | 8.107 | 12.913 | −0.626 | 10.98 | −3.98 | 11.11 | −2.772 | 11.15 | −2.42 |
| $^{281}110$ | 8.959 | 9.052 | 17.258 | 4.722 | 8.75 | 1.95 | 8.75 | 2.918 | | |
| $^{280}110$ | 9.301 | 7.679 | 16.448 | 2.531 | 9.25 | 0.33 | 9.25 | 0.9095 | | |
| $^{279}110$ | 9.601 | 8.623 | 15.797 | 2.816 | 9.89 | −1.56 | 9.89 | −0.519 | 9.84 | −0.698 |
| $^{277}110$ | 10.301 | 8.214 | 14.449 | 1.042 | 10.89 | −4.13 | 10.89 | −3.07 | | |
| $^{273}110$ | 11.369 | 7.281 | 12.834 | −1.53 | 11.67 | −5.82 | 10.30 | −1.548 | 11.37 | −3.7695 |
| $^{271}110$ | 10.871 | 6.772 | 13.587 | −1.277 | 10.90 | −4.05 | 10.38 | −1.724 | 10.899 | −2.788 |

**Table 1** (continued)

| Parent | PCM | | | | GLDM | | DDM3Y | | Experiments | |
|---|---|---|---|---|---|---|---|---|---|---|
| | $Q_\alpha$ (MeV) | $-Log\,P_0$ | -LogP | $log_{10}T^{\alpha}_{\frac{1}{2}}$ (s) | $Q_\alpha$ (MeV) | $log_{10}T^{\alpha}_{\frac{1}{2}}$ (s) | $Q^{MS}_{th}$ (MeV) | $log_{10}T^{\alpha}_{\frac{1}{2}}(Q^{MS}_{th})$ (s) | $E_\alpha$ (MeV) | $log_{10}\tau$ (s) |
| $^{270}110$ | 11.197 | 5.063 | 13.118 | −3.642 | 11.17 | −4.65 | 10.51 | 2.426 | 11.20 | −4.000 |
| $^{269}110$ | 11.586 | 6.173 | 12.608 | −2.87 | 11.28 | −4.88 | 10.84 | −2.833 | 11.58 | −3.747 |
| $^{267}110$ | 12.278 | 6.888 | 11.843 | −2.933 | 12.28 | −5.886 | 11.61 | −4.57 | 12.28 | −5.553 |
| $^{278}109$ | 9.101 | 8.8447 | 16.682 | 3.9339 | 9.58 | −0.98 | 9.58 | 0.423 | 9.55 | 7.623 |
| $^{276}109$ | 9.801 | 8.351 | 15.187 | 1.927 | 10.11 | −2.46 | 10.11 | −1.029 | 9.85 | −0.1426 |
| $^{275}109$ | 10.12 | 6.961 | 14.591 | −0.065 | 10.26 | −2.85 | 10.26 | −1.975 | 10.48 | −2.013 |
| $^{274}109$ | 10.501 | 4.296 | 13.786 | −3.544 | 10.26 | −2.83 | 10.26 | −1.395 | | |
| $^{270}109$ | 10.351 | 7.23 | 14.258 | −0.137 | 10.35 | −1.971 | 9.73 | 0.104 | 10.18 | −2.301 |
| $^{268}109$ | 10.732 | 6.791 | 13.661 | −1.182 | 10.73 | −2.893 | 10.24 | −1.264 | 10.486 | −1.678 |
| $^{276}108$ | 8.801 | 7.961 | 17.171 | 3.545 | 9.52 | −1.13 | 9.52 | −0.58 | | |
| $^{273}108$ | 9.901 | 8.409 | 14.81 | 1.604 | 9.61 | −1.36 | 9.61 | −0.399 | | |
| $^{271}108$ | 9.901 | 8.505 | 14.713 | 1.602 | 9.02 | 0.50 | 9.02 | 1.394 | | |
| $^{270}108$ | 9.299 | 7.081 | 15.994 | 1.473 | 8.88 | 0.96 | 8.88 | 1.439 | | |
| $^{269}108$ | 9.631 | 7.875 | 15.403 | 1.668 | 9.74 | −1.65 | 9.03 | 1.389 | 9.315 | 0.987 |
| $^{267}108$ | 10.121 | 7.326 | 14.500 | 0.204 | 10.12 | −1.656 | 9.53 | −0.0726 | 9.978 | −1.237 |
| $^{266}108$ | 10.337 | 5.773 | 14.14 | −1.714 | 10.21 | −2.90 | 9.88 | −1.437 | 10.336 | −2.638 |
| $^{265}108$ | 10.587 | 6.959 | 13.748 | −0.927 | 10.47 | −3.55 | 10.36 | −2.298 | | |
| $^{263}108$ | 10.671 | 7.482 | 13.647 | −0.508 | 10.67 | −4.01 | 10.91 | −3.592 | | |
| $^{274}107$ | 8.501 | 9.2958 | 17.691 | 5.4068 | 8.89 | 0.46 | 8.89 | 1.8089 | 8.8 | 54.054 |

range of superheavy nuclei [13] to study nuclear stability in this region. Therefore, the higher stability of $Z = 114$, $N = 171$ is associated with the magic numbers $Z = 114$, $N = 172$.

In all $\alpha$ decay chains in Figs. 1 and 2, at the next predicted proton number $Z = 114$, the half-lives for $N = 177$ and 179 are high in comparison with the other neutron numbers. Besides the higher stability, the two figures show a sharp change in the $\alpha$ decay half-lives for the $\alpha$ decay chains of $^{297,301,303,305}120$ at $Z = 114$ for a range of neutron numbers between 171 and 179, and it indicates that this range is close to neutron shell closure. The

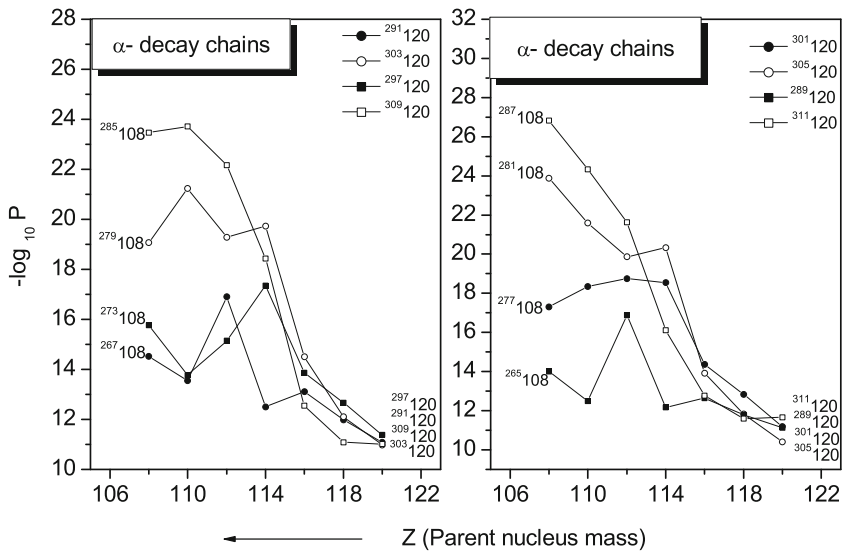


**Fig. 5** Penetration probabilities for the PCM plotted as a function of the parent nucleus' charge for the alpha decay chains of $^{291,303,297,309,301,305,289,311}120$

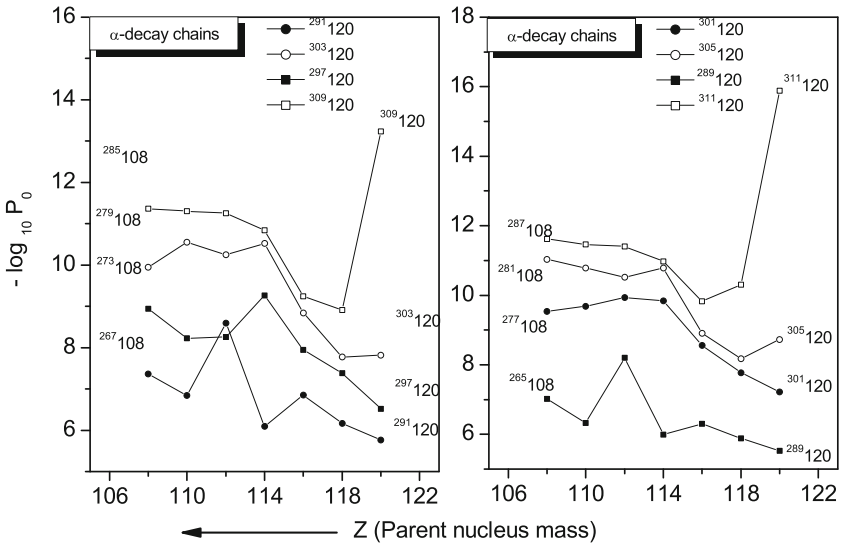


**Fig. 6** Preformation probabilities for the PCM as a function of the parent nucleus' charge for the alpha decay chains of $^{291,303,297,309,301,305,289,311}120$

largest $\alpha$ decay half-life corresponds to $Z = 114$, $N = 179$.

Figures 3 and 4 show the alpha decay energy $Q_\alpha$ as a function of charge number $Z$. In the $\alpha$ decay chains of $^{289,291,297}120$, shell effects are clearly seen, the lower decay energies reflecting the strength of the shell closures at $Z = 112$, $N = 161$; $Z = 112$, $N = 163$; and $Z = 114$, $N = 171$. In these $\alpha$ decay chains, the $Q$ values for $Z = 120$ are almost independent of the neutron number. For $Z = 108$, by contrast, the $Q$ value varies as a function of the number of neutrons. These results have been summarized in Table 1, which compares our calculated $\alpha$ decay half-lives with other model calculations and experimental data.

Figure 5 shows the penetration probability for alpha particles and all studied decay chains. The penetration probabilities of $\alpha$ decay for all considered isotopes are nearly the same at $Z = 120$, approximately $10^{-12}$. Nonetheless, they change rapidly and become markedly distinct towards lower atomic numbers. The penetration probability for $^{305}120$ exceeds that for $^{311}120$, which indicates that the nucleus with $Z = 120$, $N = 185$ is more unstable against $\alpha$ decay than the $Z = 120$, $N = 191$ nucleus. Figure 6 shows the preformation probability of $\alpha$-particles as a function of the atomic number. The parents in the $^{289}120$ $\alpha$ decay chain have the largest preformation probabilities for alpha particle in comparison with the parents of the other decay chains.

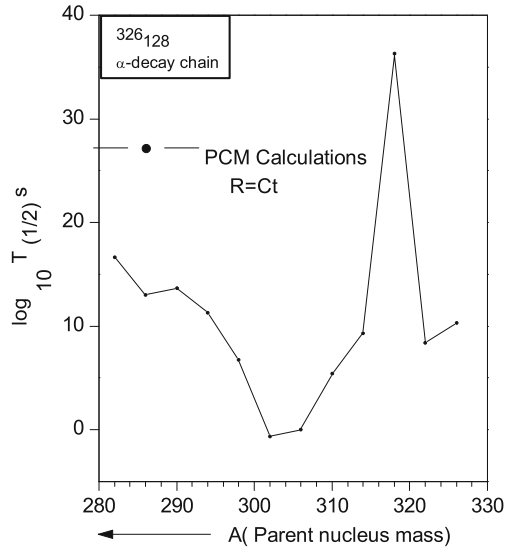


**Fig. 7** Alpha decay half-lives for the PCM as a function of the parent nucleus' charge for the $\alpha$ decay chain of $^{320}128$ ending at $^{276}106$

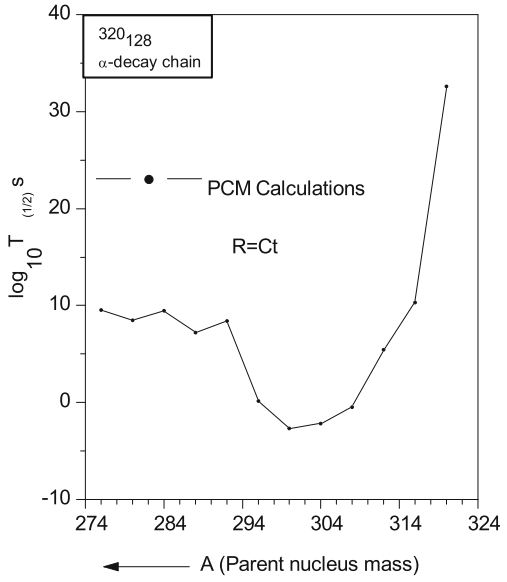


**Fig. 8** Alpha decay half-lives for the PCM as a function of the parent nucleus' charge for the $\alpha$ decay chain of $^{326}128$ ending at $^{282}106$

The preformation probability for $^{305}120$ is larger than that for the $^{311}120$ nucleus by many orders of magnitude.

### 3.2 Long-lived Superheavy Elements

Shell effects play an important role in the stability of the superheavy elements. From this viewpoint, as already mentioned, the most interesting aspect of the superheavy elements is the $\alpha$ decay chain through which they prefer to decay in comparison with spontaneous fission. To cover a mass range including the predicted neutron and proton magic numbers not covered in the above-discussed decay chains of $Z = 120$, we have performed similar calculations for other two chains. The results for the $\alpha$ decay chain of $^{326}128$, ending at $^{282}106$, is shown in Fig. 7. The most stable combination for this decay chain is $Z = 124$, $N = 194$, the half-life of which is larger than that of the parent $^{320}128$ ($Z = 128$, $N = 192$). Figure 8 shows the results for the $\alpha$ decay chain of $^{320}128$, ending at $^{276}106$. In this case, the most stable combination is $Z = 128$, $N = 192$. The half-lives for $Z = 120$, $N = 184$ is less than that for $Z = 114$, $N = 178$. The incremented stability at $Z = 114$, $N = 178$ seems due to the magicity associated with $Z = 114$, $N = 178$.

### 3.3 Possible Cluster Decay from the $^{301}120$ Decay Chain

Figures 9 and 10 show the results of our calculation for heavy cluster decay from $^{301}120$. The cluster half-lives

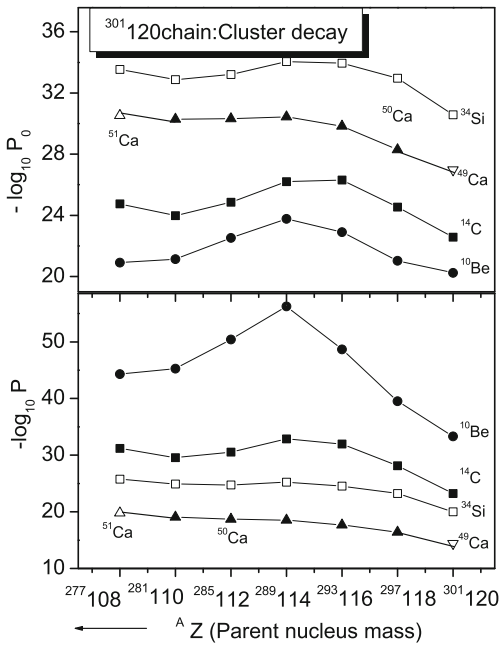


**Fig. 9** Calculated preformation penetration probabilities and penetration probabilities for different cluster decays on the basis of the PCM, for the parent nuclei of the $\alpha$ decay chain $^{301}120$

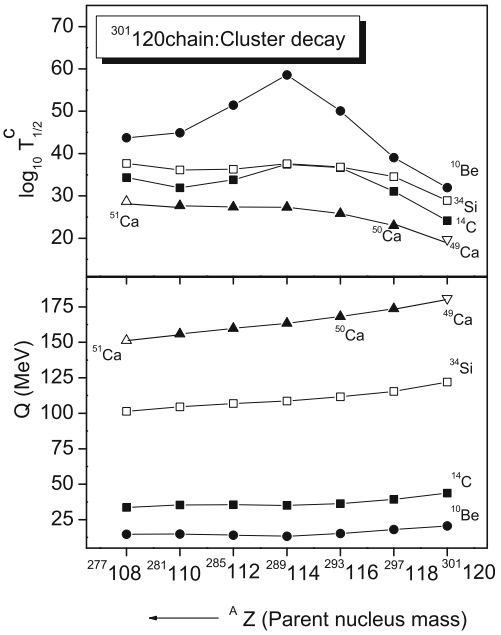


**Fig. 10** Calculated half-life and $Q$ value for different cluster decays on the basis of the PCM, for the parent nuclei belonging to the $\alpha$ decay chain $^{301}120$

are linked to the shell effects present in the daughter or in the cluster associated with the decay. For $^{301}120$, we have found $^{10}$Be to be the most probable cluster as it has the smallest penetration probability and largest preformation probability $P_0$ among the parents belonging to this particular decay chain. Even in logarithmic scales, the half-life for $^{10}$Be is much larger than the half-lives for all other clusters. All parents are therefore stable against $^{10}$Be decay. The decay of $^{10}$Be from $^{301}120$ has the daughter $Z = 116$, $N = 175$ (i. e., $^{291}116$).

Similarly, the $Q$ plots in Fig. 10 are shown for all members of the chain by considering different alternatives as the most probable clusters. The behavior of the $Q$ values are completely independent of the parent mass number. For all most probable clusters, the combination $Z = 114$, $A = 289$ has the maximum half-life against the $^{10}$Be decay, a clear consequence of shell effects. With $^{10}$Be as the most probable cluster, our study of cluster radioactivity predicts the $Z = 114$, $N = 175$ nucleus to be the most stable.

After the emission of $^{10}$Be, we considered the emission of $^{14}$C and $^{34}$Si from the parent. The cluster emission of $^{14}$C gives $Z = 114$, $N = 173$ as the daughter, while the emission of $^{34}$Si gives $Z = 106$, $N = 161$, the deformed magic nucleus $^{267}$Sg, as daughter. $^{34}$Si has the lowest preformation probability among all cases here considered. The clusters $^{49-51}$Ca have higher decay probability than the others. The decay of $^{49}$Ca from $^{301}120$ yields a deformed daughter with $Z = 100$, $N = |152$ [56].

## 4 Summary

We have studied $\alpha$ decay chains of the superheavy nuclei $^{311,309,305,303}120$, $^{301,297,291,289}120$ and $^{320,326}128$ in the preformed cluster decay model of Gupta and collaborators [35–39], which is based on quantum mechanical fragmentation theory, and compared the resulting half-lives and $Q$ values with two other model calculations (GLDM and DDM3Y) and the available experimental data. The comparison shows that our results follows the trend previously found in the model calculations. The $^{289}120$ $\alpha$ decay chain was found to have the highest preformation probability, of the order of $10^{-6}$. On the basis of the calculated half-lives and $Q$ values, we conclude that the superheavy nuclei with $Z = 112$, $N = 161, 163$; $Z = 114$, $N = 171, 178, 179$; and $Z = 124$, $N = 194$ have enhanced stability. Different cluster decays were also investigated for the $\alpha$ decay chain of $^{301}120$. Shell effects strongly increment the stability of $^{289}114$ against $^{10}$Be decay. In other cluster radioactivity calculations, the decay of $^{34}$Si from the parent $^{301}120$ yields a deformed magic daughter with $Z = 106$ and $N = 161$, and the decay of $^{49}$Ca from the same parent yields another deformed magic nucleus, with $Z = 100$ and $N = 152$.

## References


1. W.D. Myers, W.J. Sewiatecki, Nucl. Phys. **1**, A81 (1966)
2. A. Sobiczewski, F.A. Gareev, B.N. Kalinkin, Phys. Lett. **500**, 22 (1966)
3. H. Meldner, Ark. Fys. **593**, 36 (1967)
4. S.G. Nilsson et al., Nucl. Phys. **545**, A115 (1968)
5. U. Mosel, W. Greiner, Z. Phys. **261**, 222 (1969)
6. J. Grumann, U. Mosel, B. Frink, W. Greiner, Z. Phys. **371**, 228 (1969)
7. S.G. Nilsson, C.F. Tsang, A. Sobiczewski, Z. Szymanski, S. Wyeech, C. Gustafsson, I.L. Lamm, P. Möller, B. Nilsson, Nucl. Phys. **1**, A131 (1969)
8. E.O. Fiset, J.R. Nix, Nucl. Phys. **647**, A193 (1972)
9. J. Randrup, S.E. Larsson, P. Möller, A. Sobiczewski, A. Lukasiak, Phys. Scr. **10A**, 60 (1974)
10. A. Sobiczewski, Phys. Part. Nucl. **295**, 25 (1994)
11. R. Smolanczuk, J. Skalski, A. Sobiczewski, Phys. Rev. **1871**, C52 (1995)
12. P. Möller, J.R. Nix, J. Phys. G: Nucl. Part. Phys. **1681**, 20 (1994)
13. K. Rutz, M. Bender, T. Bürvenich, T. Schilling, P.G. Reinhard, J.A. Maruhn, W. Greiner, Phys. Rev. **238**(C56) (1997)
14. S. Cwiok, J. Dobaczewski, P.H. Heenen, P. Magierski, W. Nazarewicz, Nucl. Phys. **211**, A611 (1996)
15. R.K. Gupta, G. Müenzenberg, W. Greiner, J. Phys. G: Nucl. Part. Phys. **L13**, 23 (1997)
16. A.A. Saldanha, A.R. Farhan, M.M. Sharma. J. Phys. G: Nucl. Part. Phys. **115103**(36) (2009)
17. S. Kumar, Phys. Rev. **024320**, C85 (2012)
18. G.G. Adamian, N.V. Antonenko, W. Scheid, Acta Phys. Polon. **737**, B40 (2009)
19. H.F. Zhang, Y. Gao, N. Wang, J.Q. Li, E.G. Zhao, G. Royer, Phys. Rev. **014325**, C85 (2012)
20. S. Kumar, S. Thakur, R. Kumar, J. Phys. G. **105104**, 36 (2009)
21. S. Hofmann, Rep. Prog. Phys. **639**(61) (1998)
22. Y.T. Oganessian et al., Phys. Rev. Lett. **3154**, 83 (1999)
23. Y.T. Oganessian et al., Phys. Rev. **011301(R)**(C63) (2001)
24. Y.T. Oganessian et al., Phys. Rev. **041604(R)**(C62) (2000)
25. Y.T. Oganessian et al., Phys. Rev. Lett. **142502**(104) (2010)
26. S. Kumar, M. Balasubramanium, R.K. Gupta, G. Münzenberg, W. Scheid, J. Phys. G: Nucl. Part. Phys. **625**(29) (2003)
27. C.H.E.N. Bao-Qiu et al., Chin. Phys. Lett. **22**(2), 302 (2005)
28. V.I. Zagrebaev, W. Greiner, Phys. Rev. **044618**, C83 (2011)
29. V.I. Zagrebaev, A.V. Karpov, I.N. Mishustin, W. Greiner, Phys. Rev. **044617**, C84 (2011)
30. S. Cwiok, A. Sobiczewski, Z. Phys. **203**, A342 (1992)
31. R. Smolanczuk, Phys. Rev. **812**, C56 (1997)
32. D.N. Poenaru, R.A. Gherghescu, W. Greiner, Phys. Rev. Lett. **062503**, 107 (2011)
33. D.N. Poenaru, R.A. Gherghescu, W. Greiner, Phys. Rev. **034615**, C85 (2012)
34. V.I. Zagrebaev, A.V. Karpov, W. Greiner, Phys. Rev. **044608**, C81 (2010)
35. S.S. Malik, R.K. Gupta, Phys. Rev. **C, 1992**(39) (1989)
36. R.K. Gupta, W. Scheid, W. Greiner, J. Phys. G. **1731**, 17 (1991)
37. S. Kumar, R.K. Gupta, Phys. Rev. **C,1922**, 49 (1994)
38. R.K. Gupta, in *Heavy Elements and Related New Phenomena*, ed. by W. Greiner, R.K. Gupta. World Scientific, Singapore, vol. II, (1999), p. 730
39. R.K. Gupta, Rev, Phys. C. **1278**, 21 (1980)
40. R.K. Gupta, W. Greiner, in *Heavy Elements and Related New Phenomena,* vol. I, ed. by W. Greiner, R.K. Gupta. (World Sc., 1999), p. 397
41. J. Maruhn, W. Greiner, Phys. Rev. Lett. **548**, 32 (1974)
42. R.K. Gupta, W. Scheid, W. Greiner, Phys. Rev. Lett. **353**, 35 (1975)
43. R.K. Gupta, C. Pârvulescu, A. Săndulescu, W. Greiner, Z. Physik. **217**, A283 (1977)
44. R.K. Gupta, A. Săndulescu, W. Greiner, Z. Naturforsch. **704**, 32a (1977)
45. R.K. Gupta, Sovt. J. Part. Nucl. **289**, 8 (1977)
46. R.K. Gupta, Nucl. Phys. Solid St. Phys. Symp. (India). **171**, 21A (1978)
47. R.K. Gupta, in *Proc. 5th Int. Conf. on Nuclear Reaction Mechanisms,* Varenna, (1988), p. 416
48. R.K. Gupta, in *ibid* [40]. vol. II, p. 730
49. J. Blocki et al., Ann. Phys. (NY). **427**, 105 (1977)
50. G. Audi, A.H. Wapstra, C. Thibault, Nucl. Phys. **337**, A729 (2003)
51. P. Möller, J.R. Nix, W.D. Myers, W.J. Swiatecki, At. Data Nucl. Data Tables. **185**, 59 (1995)
52. H. Kröger, W. Scheid, J. Phys. G, **L85**, 6 (1980)
53. G. Royer, R.A. Gherghesu, Nucl. Phys. **479**, A 699 (2002)
54. Y.T. Oganessian, Pure Appl. Chem. **78**(5), 889–904 (2006)
55. S. Hofmann, G. Münzenberg, Rev. Mod. Phys. **733**, 72 (2000)
56. Yu. A. Lazarev et al., Phys. Rev. C **620**, 54 (1996)